

Temperature-dependent hardness of diamond-structured covalent materials

Xing Feng¹, Jianwei Xiao¹, Bin Wen^{1,*}, Jijun Zhao², Bo Xu^{1,†}, Yanbin Wang³, Yongjun Tian¹

¹Center for High Pressure Science, State Key Laboratory of Metastable Materials Science and Technology, Yanshan University, Qinhuangdao 066004, China

² Key Laboratory of Materials Modification by Laser, Ion and Electron Beams (Ministry of Education), Dalian University of Technology, Dalian 116024, China

³Center for Advanced Radiation Sources, University of Chicago, Chicago, Illinois 60439, USA.

Abstract Understanding temperature-dependent hardness of covalent materials is not only of fundamental scientific interest, but also of crucial importance for technical applications. In this work, a temperature-dependent hardness formula for diamond-structured covalent materials is constructed on the basis of the dislocation theory. Our results show that, at low temperature, the Vickers hardness is mainly controlled by Poisson's ratio and shear modulus with the latter playing a dominant role. With increasing temperature, the plastic deformation mechanism undergoes a transition from shuffle-set dislocation control to glide-set dislocation control, leading to a steeper drop of hardness at high temperature. In addition, an intrinsic parameter, a^3G , is revealed for diamond-structured covalent materials, which measures the resistance to soften at high temperature. Our hardness model shows remarkable agreement with experimental data. Current work not only sheds lights on the physical origin of hardness, but also provides a direct principle for superhard materials design.

Authors to whom any correspondence should be addressed

* E-mail address: wenbin@ysu.edu.cn (Bin Wen)

† E-mail address: bxu@ysu.edu.cn (Bo Xu)

Hardness measures the ability of a material to resist plastic deformation induced by indentation or scratching of another material [1]. In the past decades, many theoretical investigations have been carried out to study the hardness of materials and several theoretical or semi-empirical hardness formulas have been established for covalent materials [2-8]. These hardness formulas can well reproduce a material's intrinsic Vickers hardness, and they are used to design superhard materials and have varying degrees of success [9]. For example, by using Chen's formulas [8], a perfect correspondence between the calculated and experimental values of hardness can be achieved for a wide variety of crystalline materials as well as bulk metallic glasses.

Note these hardness models are established for the ambient conditions where temperature effect is usually ignored. In reality, materials are usually processed or operated in variable temperature condition, and their properties under high temperature are vital for practical applications. Therefore, the study of temperature-dependent hardness becomes of interest in many fields [10], such as, modeling the mechanical behavior of materials in technological processes, assessing the performance of tools under high temperature conditions, etc. Experimentally, it is difficult to carry out temperature-dependent hardness measurements due to complexity of sample preparation and maintaining the sample under high temperature conditions, and these difficult lead to high measurements error. Even though this, it is indicated that the hardness of diamond-structured covalent materials is softening with increasing temperature and there exist a steeper drop of hardness at high temperature [1,11-15], and a reasonable theoretical explanation is needed for these experimental results. Theoretically, the temperature effect on hardness were previously considered with parameters determined from experimental data fitting [1,10]. Still, the physical insights behind the temperature effect, such as the contributions from dislocation characteristics, microstructure, and

loading conditions, have not been explored, and the universality and portability to other materials systems are questionable. It is urgently needed to establish a temperature-dependent hardness model that can reflect dislocation characteristic, microstructure and loading conditions effect on hardness now.

Experiments indicate that plastic deformation takes place in the hardness tests of covalent materials, and this plastic deformation is related with their dislocation behavior [1]. Recent theoretical study [16] also indicated that the hardness of covalent materials is also controlled by their dislocation behavior. Because dislocation motion is a thermally activated process [17], temperature, dislocation characteristic, microstructure and loading conditions effect on hardness can be considered in modeling hardness by involving dislocations. In this study, we report a temperature-dependent hardness formula for diamond-structured covalent materials based on dislocation theory.

The main dislocation slip systems for diamond-structured covalent materials are of $\{111\}\langle 110\rangle$ type [16,18]. Due to the two-interpenetrating face-centered crystal (fcc) sublattices, dislocation slips on $\{111\}$ planes can occur at two different glide planes, *i.e.*, glide-set and shuffle-set glide planes (Fig. 1a). Usually, a $\frac{1}{2}\langle 110\rangle$ glide-set dislocation can be dissociated into two $\frac{1}{6}\langle 112\rangle$ glide-set partial dislocations. In contrast, a $\frac{1}{2}\langle 110\rangle$ shuffle-set dislocation would stay intact due to excessively high energy required for the dissociation. Meanwhile, the strong directional covalent bonds in diamond-structured materials result in a large Peierls barrier with deep trough along $\langle 110\rangle$ directions, limiting the dislocation lines along these directions [16,19]. Therefore, two types of dislocations, namely the $\frac{1}{6}\langle 112\rangle$ glide-set 90° partial (edge) dislocations and $\frac{1}{2}\langle 110\rangle$ shuffle-set perfect (screw) dislocations, dominate the plastic deformation in diamond-structured covalent materials, as indicated in Fig. S1 of Supplemental Information (SI). These dislocations

propagate primarily through kinks, or specifically through kink pairs that are the most favorable way for kink motion [20], as illustrated in Fig. 1b.

The total energy (W) of a kink-pair as a function of kink-pair width (x) and applied shear stress (τ) contains four terms: the kink formation energy ($2W_f$), kink migration energy (W_m), kink-pair interaction energy (W_{int}), and work done by the applied stress (W_τ). On the basis of dislocation theory [17], W can be expressed as

$$W(x, \tau) = 2W_f + W_m + W_{\text{int}} + W_\tau = \frac{A_1 G b^2 h}{2\pi} \ln\left(\frac{R}{r}\right) + W_m - \frac{A_2 G b^2 h^2}{8\pi x} - hb x \tau, \quad (1)$$

where b is the magnitude of Burgers vector, h the kink height, G the shear modules, R the integral range of linear elasticity theory, r the radius of dislocation core, $A_1 = \cos^2 \beta + \frac{\sin^2 \beta}{1-\nu}$ and $A_2 = \frac{(1+\nu)\cos^2 \beta + (1-2\nu)\sin^2 \beta}{1-\nu}$ with ν being Poisson's ratio and β the angle between Burgers vector and the dislocation line.

As shown in Fig. 1c, W as a function of x oscillates with the lattice periodicity along $\langle 110 \rangle$ direction. The envelope of the local maxima forms a curve (dashed line in Fig. 1c), and the maximum of the envelope can be considered as the activation energy of dislocation motion. Mathematically, the critical kink-pair width corresponding the activation energy, x_c , can be determined with the first derivative test [17]. Note W_m contributing to the local variation (oscillation) can be ignored when considering the envelope maximum. As a result,

$$x_c = \left(\frac{A_2 h b G}{8\pi \tau} \right)^{1/2}, \quad (2)$$

and the activation energy as a function of τ can then be determined as

$$W_c(\tau) = \frac{A_1 G b^2 h}{2\pi} \ln\left(\frac{x_c}{r}\right) - (hb)^{3/2} \left(\frac{A_2 G \tau}{2\pi}\right)^{1/2}. \quad (3)$$

Here R in Eq. 1 is set as x_c for an approximation. The calculated activation energies as a function of applied shear stress for $\frac{1}{6}\langle 112 \rangle$ glide-set 90° partial dislocation and $\frac{1}{2}\langle 110 \rangle$ shuffle-set perfect dislocation are shown in Fig. 1d, where a crossover is clearly revealed with increasing shear stress, indicating a competition of deformation mechanism between glide-set and shuffle-set dislocations. This result based on the dislocation theory is further confirmed by the molecular dynamics (MD) simulation for diamond (inset of Fig. 1d, also see SI part I for MD calculation detail), and is consistent with previous experimental observations [11].

The dislocation motion is controlled by both applied shear stress and thermal activation [17]. For a given set of temperature T , applied stress τ , and plastic strain rate $\dot{\epsilon}$, the temperature-dependent critical shear stress can be written with a transcendental equation based on Eq. 3 and Orowan's relation [17] as following,

$$\tau_c^T = \frac{2\pi}{A_2 h^3 b^3 G} \left[\frac{A_1 G b^2 h}{2\pi} \ln\left(\frac{x_c}{r}\right) - k_B T \ln\left(\frac{\rho_m b \lambda_b \nu_D}{\dot{\epsilon}}\right) \right]^2, \quad (4)$$

where k_B is the Boltzmann constant, ρ_m the density of mobile dislocations, λ_b the mean free path of dislocations slipping over obstacles, and ν_D the Debye frequency. By substituting Eq. (2) into Eq. (4), we have

$$\frac{\tau_c^T}{G} = C_1 \left[C_2 \ln\left(C_3 \frac{G}{\tau_c^T}\right) - \frac{k_B T}{a^3 G} \ln\left(\frac{\rho_m b \lambda_b \nu_D}{\dot{\epsilon}}\right) \right]^2, \quad (5)$$

where $C_1 = \frac{2\pi a^6}{h^3 b^3 A_2}$, $C_2 = \frac{h b^2 A_1}{4\pi a^3}$, and $C_3 = \frac{h b A_2}{8\pi r^2}$ are dimensionless constants only related to

Poisson's ratio of the materials and the geometry of involved dislocation. a is the lattice parameter.

Table 1 lists the information for $\frac{1}{6}\langle 112 \rangle$ glide-set 90° dislocation and $\frac{1}{2}\langle 110 \rangle$ shuffle-set 0° perfect dislocation. Others parameters, such as temperature-dependent lattice constant, shear modulus, and Poisson's ratio, *etc.*, were determined with the methods presented in Refs. [21-23] (see

SI part II for calculation details). These parameters at 0 K are listed in Table 2. The temperature-dependent critical shear stresses, $\tau_{c,s}^T$ for shuffle-set dislocation and $\tau_{c,g}^T$ for glide-set one, can then be evaluated from Eq. (5) with a geometric or numerical method. These two types of dislocations compete with each other, and the one with lower critical shear stress dominates the deformation at given temperature and shear stress. Therefore, the critical shear stress of the investigated materials can be determined as

$$\hat{\tau}_c^T = \min(\tau_{c,s}^T, \tau_{c,g}^T). \quad (6)$$

Usually, the strength of a diamond-structured covalent material is characterized by its hardness. The Vickers hardness of diamond-structured covalent material is about 2.74 times of the yield strength [24], and the yield strength is roughly 3.1 (Taylor factor for an fcc structure) times of the critical shear stress [25]. Therefore, the temperature dependent Vickers hardness for diamond-structured covalent materials can be estimated as

$$H_T \approx 8.5\hat{\tau}_c^T. \quad (7)$$

Fig. 2a displayed the calculated Vickers hardness (at 300 K) for typical diamond-structured covalent materials compared with the experimental data [8], exhibiting a nice consistency. The temperature-dependent Vickers hardness of diamond, Si and Ge are calculated and plotted in Fig. 2b–d (see Fig. S2 for the temperature-dependent lattice constant, shear moduli, and Poisson's ratio), respectively, in good accordance with the experimental hardness values over a wide temperature range [1,12-15]. In addition, the calculated transition temperatures from the shuffle-set dislocation controlled deformation to glide-set dislocation controlled one (T_{s-g}) are 1402.6 K, 676.8 K and 560.2 K for diamond, Si and Ge, respectively, which are comparable with the experimental values, *i.e.*, 1450 K for diamond [11], 650 K for Si [1], and 600 K for Ge [15].

At low temperature, the dislocation motions due to thermal activation can be ignored. In this case, the Vickers hardness determined from Eqs. (5)–(7) for a diamond-structured covalent material is determined by the shear modulus and Poisson’s ratio, and Eq. (7) can be simplified as

$$H_0 = k_0(\nu)G, \quad (8)$$

where $k_0(\nu)$ is a proportional coefficient related to Poisson’s ratio. Fig. 3 shows the Vickers hardness map at 0 K constructed from Eq. (7). Obviously, both shear modulus and Poisson’s ratio contributes to the Vickers hardness. As shown in Fig. 3b, the Vickers hardness increase linearly with increasing shear modulus, and $k_0(\nu)$ decreases slightly with increasing Poisson’s ratio. Compared with shear modulus, Poisson’s ratio shows a less prominent effect on the Vickers hardness (Fig. 3c). It is clear that high shear modulus and low Poisson’s ratio are essential for (super)hard materials. In addition, we note that the proportional coefficient $k_0(\nu)$ varies in a narrow range of 0.14–0.19 for ν in the range of 0–0.3 (see the inset of Fig. 3a). By fitting $k_0(\nu)$ with ν , Eq. 8 can be rewritten as

$$H_0 = (0.18 + 0.05\nu - 0.51\nu^2)G. \quad (9)$$

Previously, some semi-empirical hardness models relating hardness to materials’ shear modulus directly with proportional coefficients of 0.12 [1], 0.151 [2], 0.147 [7] fitted from experimental data. These values agree nicely with $k_0(\nu)$ calculated in current work, verifying the effectiveness of our consideration of hardness on the basis of dislocation dynamics.

At elevated temperature, the thermal activated dislocation motions start to function. From Eq. (5), τ_c^T/G is clearly correlated with Poisson’s ratio, temperature, and a materials-related parameter of a^3G , which combined with Eq. (7) gives the temperature dependent Vickers hardness as

$$H = k(T, a^3G, \nu)G, \quad (10)$$

with the proportional coefficient k as a function of ν , T and a^3G . The thermal and material's non-elastic properties effects are essentially included in k . Note that $k = H/G$ can be considered as a normalized hardness with respect to material's shear modulus.

Fig. 4 shows k as a function of ν , T and a^3G . Considering the general range of ρ_m , λ_b , and $\dot{\epsilon}$ for interested materials (such as those listed in Table 1), we find the estimated values of the second logarithm in Eq. 5, $\ln\left(\frac{\rho_m b \lambda_b v_D}{\dot{\epsilon}}\right)$, vary in a relatively narrow range for different diamond-structured covalent materials (Fig. S3). Therefore, fixed values of 18.8 and 32.1 are used in the calculation for shuffle-set and glide-set dislocations, respectively. Similar simplification was previously used [26]. As shown in Fig. 4a, k decreases with increasing temperature for a given set of Poisson's ratio and a^3G , indicating softening occurs at high temperature. Furthermore, for a fixed Poisson's ratio, the larger a^3G is, the slower k decreases, indicating that materials with larger a^3G are more difficult to soften with increasing temperature. The transition temperature T_{s-g} from shuffle-set dislocation control to glide-set dislocation control is calculated and shown in Fig. 4b. T_{s-g} increases linearly with a^3G for a given Poisson's ratio, meanwhile it goes to higher temperature with larger Poisson's ratio. It is justified to identify a^3G as an intrinsic index for diamond-structured covalent materials, measuring the resistance to soften at elevated temperature, which is consistent with previous semi-empirical results [27].

Besides the above-mentioned intrinsic properties that determine hardness of materials, other factors, such as dislocation characteristic, microstructure and loading conditions of the sample, *etc.*, also show great impact on the hardness. These additional effects can easily be accounted for in current dislocation-based hardness model (Fig. S4). For example, the hardness varies with the density of mobile dislocations: the larger the dislocation density, the lower the hardness (Fig. S4a).

The effects of loading speed (Fig. S4b) and grain boundary (Fig. S4c) on hardness have also been investigated.

In summary, a temperature-dependent Vickers hardness model has been developed on the basis of dislocation theory for diamond-structured covalent materials. At low temperature, the Vickers hardness is mainly controlled by Poisson's ratio and shear modulus with the latter playing a dominant role. At elevated temperature, the deformation mechanism changes from shuffle-set dislocation control to glide-set dislocation control, and the Vickers hardness is further affected by temperature and a material-related parameter of a^3G . Materials with larger a^3G are more difficult to soften at elevated temperature. These findings help to unveil the physics of hardness, and can provide a direct guidance for superhard materials design, especially at high temperature.

Acknowledgment

This work was supported by the National Natural Science Foundation of China (Grant Nos. 51771165, and 51525205), National Magnetic Confinement Fusion Energy Research Project of China (2015GB118001) and NSF (Grant No. EAR-1361276) and the National Key R&D Program of China (YS2018YFA070119).

References

- [1] J. J. Gilman, *Chemistry and Physics of Mechanical Hardness* (John Wiley & Sons, 2009), Vol. 5.
- [2] D. M. Teter, *Mrs Bulletin* **23**, 22 (1998).
- [3] F. Gao, J. He, E. Wu, S. Liu, D. Yu, D. Li, S. Zhang, and Y. Tian, *Physical Review Letters* **91**, 015502 (2003).
- [4] Z. Ding, S. Zhou, and Y. Zhao, *Physical Review B* **70**, 3352 (2004).
- [5] A. Šimůnek and J. Vackář, *Physical Review Letters* **96**, 085501 (2006).
- [6] K. Li, X. Wang, F. Zhang, and D. Xue, *Physical Review Letters* **100**, 235504 (2008).
- [7] X. Jiang, J. Zhao, and X. Jiang, *Computational Materials Science* **50**, 2287 (2011).
- [8] X. Q. Chen, H. Niu, D. Li, and Y. Li, *Intermetallics* **19**, 1275 (2011).
- [9] A. Mansouri Tehrani and J. Brgoch, *Journal of Solid State Chemistry* **271**, 47 (2019).
- [10] V. A. Mukhanov, O. O. Kurakevych, and V. L. Solozhenko, *Philosophical Magazine* **89**, 2117 (2009).
- [11] D. J. Weidner, Y. Wang, and M. T. Vaughan, *Science* **266**, 419 (1994).
- [12] N. V. Novikov, Y. V. Sirota, V. I. Mal'Nev, and I. A. Petrusha, *Diamond & Related Materials* **2**, 1253 (1993).
- [13] T. Suzuki and T. Ohmura, *Philosophical Magazine A* **74**, 1073 (1996).
- [14] V. Trefilov and Y. V. Mil'Man, *Soviet Physics Doklady* **8** (1964).
- [15] A. P. Gerck, *Philosophical Magazine* **32**, 355 (1975).
- [16] J. Xiao, H. Yang, X. Wu, F. Younus, P. Li, B. Wen, X. Zhang, Y. Wang, and Y. Tian, *Science Advances* **4** (2018).
- [17] J. P. Hirth, J. Lothe, and T. Mura, *Theory of Dislocations (2nd ed.)* (Wiley, 1983).

- [18] A. T. Blumenau, M. I. Heggie, C. J. Fall, R. Jones, and T. Frauenheim, *Physical Review B* **65**, 205205 (2002).
- [19] H. Yang, J. Xiao, Z. Yao, X. Zhang, F. Younus, R. Melnik, and B. Wen, *Diamond and Related Materials* **88**, 110 (2018).
- [20] H. Kolar, J. Spence, and H. Alexander, *Physical Review Letters* **77**, 4031 (1996).
- [21] T. Shao, B. Wen, R. Melnik, S. Yao, Y. Kawazoe, and Y. Tian, *Journal of Applied Physics* **111**, 083525 (2012).
- [22] B. Wen, T. Shao, R. Melnik, Y. Kawazoe, and Y. Tian, *Journal of Applied Physics* **113**, 103501 (2013).
- [23] X. Feng, J. Xiao, R. Melnik, Y. Kawazoe, and B. Wen, *The Journal of Chemical Physics* **143**, 104503 (2015).
- [24] A. P. Sekhar, S. Nandy, K. K. Ray, and D. Das, in *IOP Conference Series: Materials Science and Engineering* (IOP Publishing, 2018).
- [25] R. E. Stoller and S. J. Zinkle, *Journal of Nuclear Materials* **283-287**, 349 (2000).
- [26] Z. S. Basinski, *Philosophical Magazine* **4**, 393 (1959).
- [27] H. Siethoff, *Journal of Applied Physics* **94**, 3128 (2003).
- [28] V. V. Brazhkin, A. G. Lyapin, and R. J. Hemley, *Philosophical Magazine A* **82**, 231 (2002).
- [29] M. L. Williams, *Occupational & Environmental Medicine* **126**, 81 (1996).
- [30] A. Szymański and J. M. Szymański, *Hardness Estimation of Minerals Rocks & Ceramic Materials* (1989).
- [31] C. M. Sung and M. Sung, *Materials Chemistry & Physics* **43**, 1 (1996).

Table 1. Geometric parameters for $\frac{1}{6}\langle 112 \rangle$ glide-set 90° partial and $\frac{1}{2}\langle 110 \rangle$ shuffle-set perfect dislocations.

Dislocation type	β	b	h	r	ρ_m (m ⁻²)	λ_b (nm)	$\dot{\epsilon}$ (s ⁻¹)
$\frac{1}{2}\langle 110 \rangle$ shuffle-set	0°	$\sqrt{2}a/2$	$\sqrt{6}a/4$	$0.9b$	0.3×10^8	100	10^{-4}
$\frac{1}{6}\langle 112 \rangle$ glide-set	90°	$\sqrt{6}a/6$	$\sqrt{6}a/4$	$0.3b$	0.3×10^{14}	100	10^{-4}

Table 2. Calculated lattice constants, shear moduli, α^3G , Poisson's ratios, Debye frequencies at 0 K and shuffle-set to glide-set transition temperatures for selected diamond-structured covalent materials, in comparison with experimental ones, and their corresponding transition temperature. Hardness values are given for temperatures (0 K and 300 K).

Phase	a (Å)	G (GPa)	α^3G ($\times 10^{-18}$ J)	ν	ν_D (THz)	H_0 (GPa)	$H_{300\text{ K}}$ (GPa)	H_{exp} (GPa)	$T_{\text{s-g}}$ (K)
Diamond	3.57	521	23.7	0.07	39.3	94.7	85.6	60-150 ^a	1402.6
Si	5.47	64.2	10.5	0.21	15.1	10.9	8.9	11.3 ^b	676.8
Ge	5.78	45	8.7	0.19	8.3	7.8	6.1	7.2 ^c	560.2
AlAs	5.73	43.86	8.3	0.23	11.3	7.3	5.6	5 ^d	542.8
AlP	5.51	52	8.7	0.24	12.9	10.7	8.9	9.4 ^d	722.5
AlSb	6.23	32	7.7	0.23	9.8	5.3	4	4 ^d	509.7
BAs	4.82	129.4	14.5	0.13	21.4	23.1	19.8	19 ^b	886.4
BN	3.63	390	18.7	0.11	34.2	70.2	62.0	46-80 ^a	1125.5
BP	4.55	168	15.8	0.11	24.0	30.2	26.1	31 ^a	957.9
GaAs	5.76	43.68	8.3	0.22	7.7	7.3	5.8	7.5 ^b	550.4
GaP	5.53	54	9.1	0.22	10.8	9.1	7.2	9.5 ^d	597.4
GaSb	6.22	32.2	7.7	0.21	6.4	6.7	5.4	4.5 ^d	625.7
InAs	6.21	28.3	6.8	0.26	6.2	4.5	3.3	3.8 ^d	463.6
InP	6	34.1	7.4	0.26	9.4	5.5	4.1	5.4 ^d	498.7
InSb	6.65	22.28	6.6	0.25	5.0	3.6	2.7	2.2 ^d	445.9
SiC	4.38	198.74	16.7	0.14	24.1	33.4	29.4	26-37 ^a	1076.4

^a Vickers hardness from Ref. [28]

^b Knoop hardness from Ref. [29]

^c Vickers hardness from Ref. [30]

^d Knoop hardness from Ref. [31]

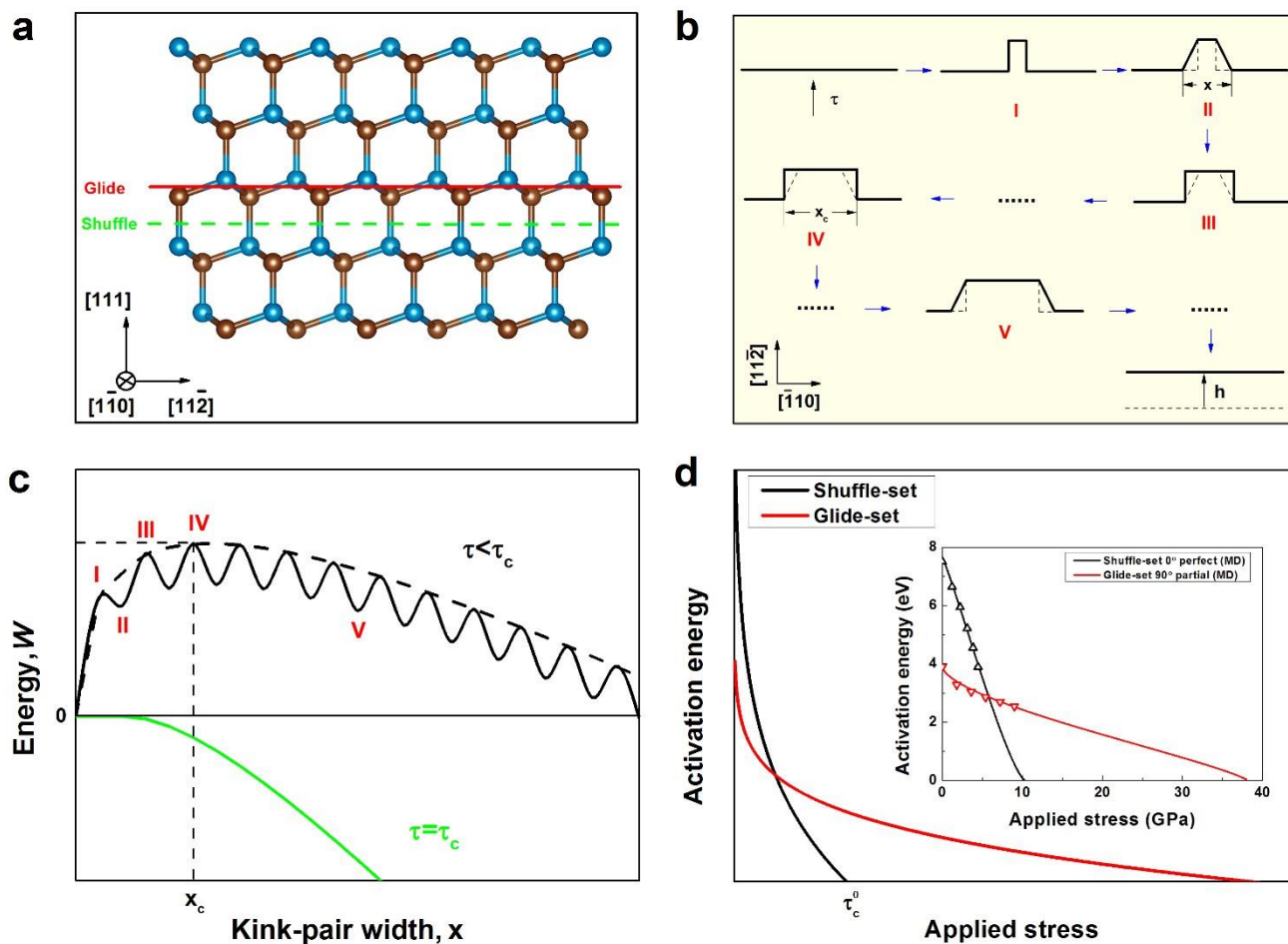


Fig. 1. Schematic diagram for the computational method used in this study. (a) $\{110\}$ projection of the diamond-structured lattice. The green and red lines indicate the $\{111\}$ shuffle and glide planes, respectively. (b) Kink-pair nucleation and motion process under applied stress. Shear stress τ acting perpendicularly to a dislocation line parallel to $[\bar{1}10]$ produces a kink pair (I), which expands subsequently (II through V), resulting in an upward motion of the dislocation line in $[11\bar{2}]$ direction with a step of h . (c) Total energy variation with respect to kink-pair width under different applied shear stress conditions. The oscillation reflects lattice periodicity. (d) Activation energy as a function of applied stress for shuffle-set and glide-set dislocation motion. The inset shows the MD result for diamond.

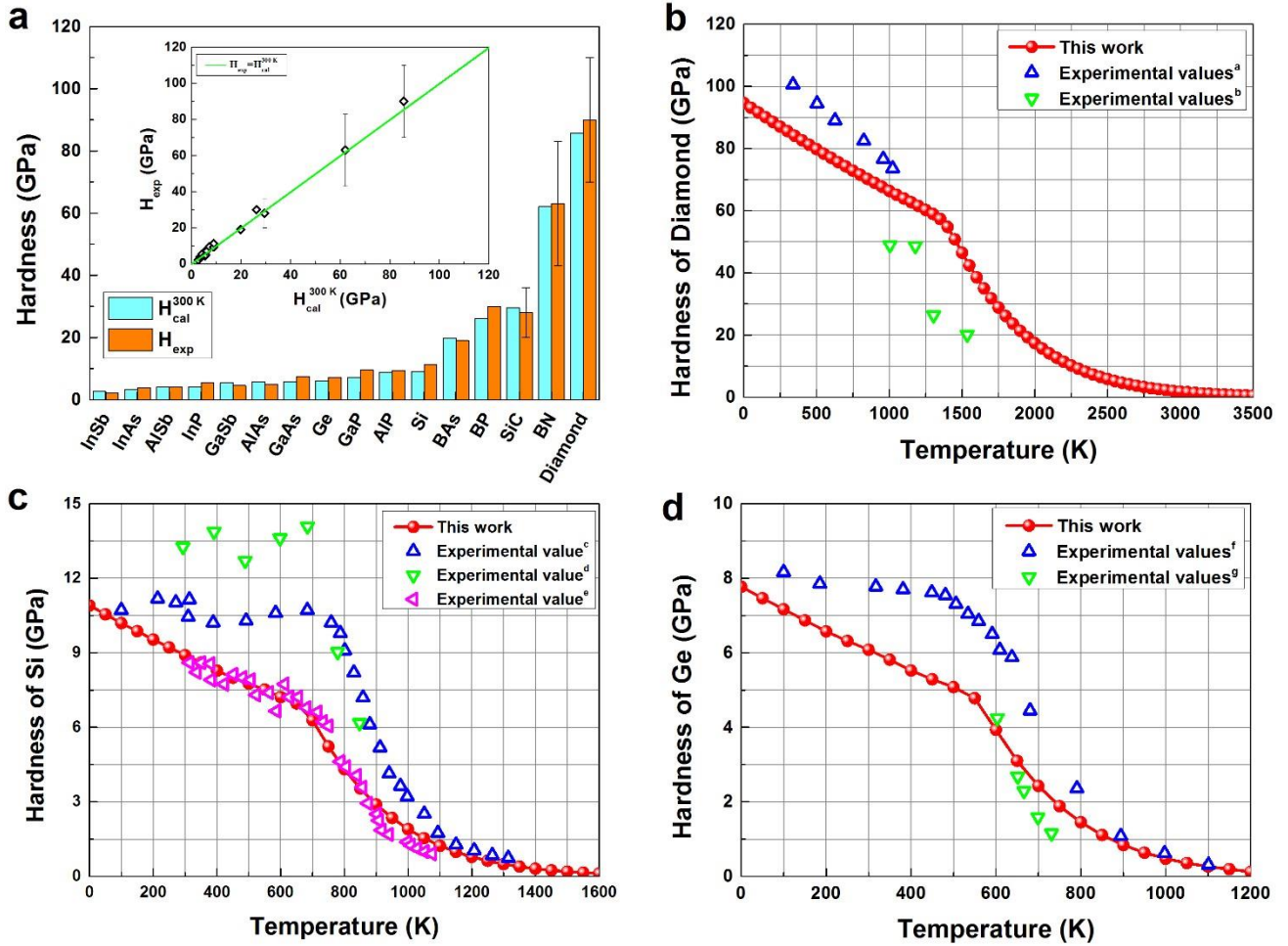


Fig. 2. Calculated Vickers hardness compared with experimental values. (a) Comparison of Vickers hardness values from current work and experimental results at 300 K. (b–d) Calculated temperature dependent Vickers hardness for diamond, Si, and Ge in comparison with experimental data (^aRef. [12], ^bRef. [11], ^cRef. [13], ^dRef. [14], ^eRef. [1], ^fRef. [15], ^gRef. [14]).

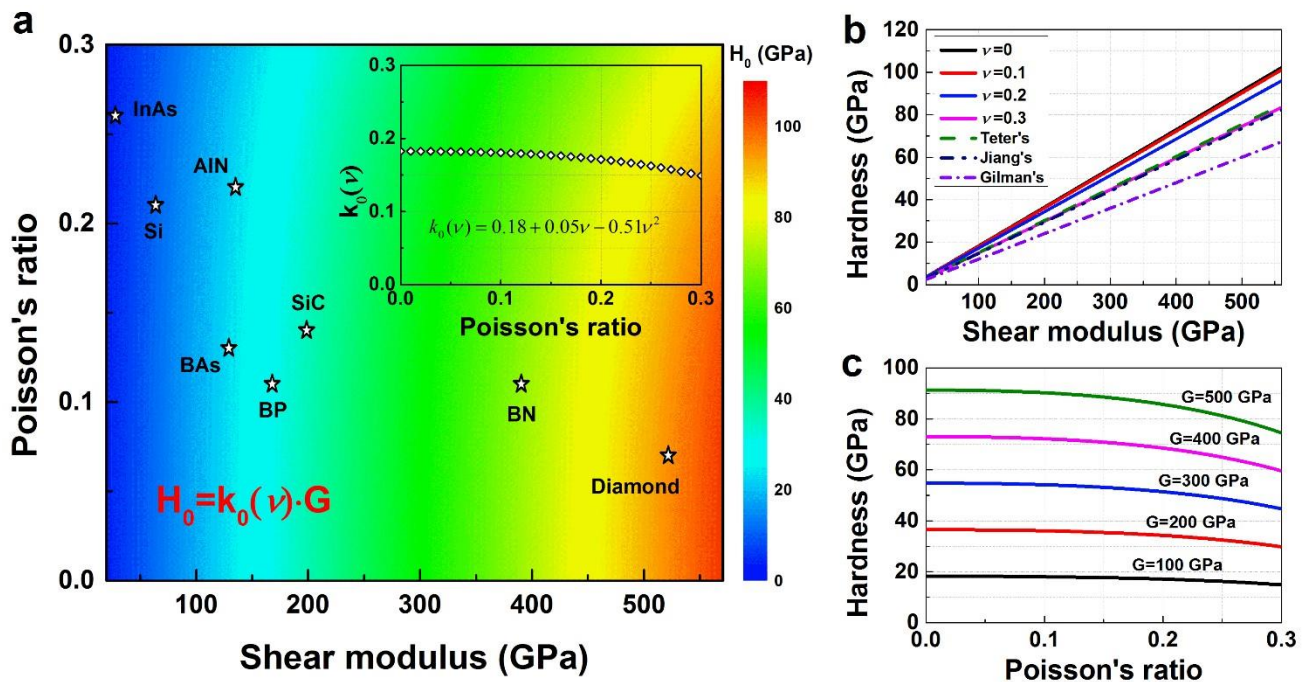


Fig. 3. Effect of shear modulus and Poisson's ratio on hardness of diamond-structured covalent materials at 0 K. (a) Calculated Vickers hardness map as a function of shear modulus and Poisson's ratio. (b) Effect of shear modulus on materials hardness with different Poisson's ratio. (c) Effect of Poisson's ratio on materials hardness with different shear modulus.

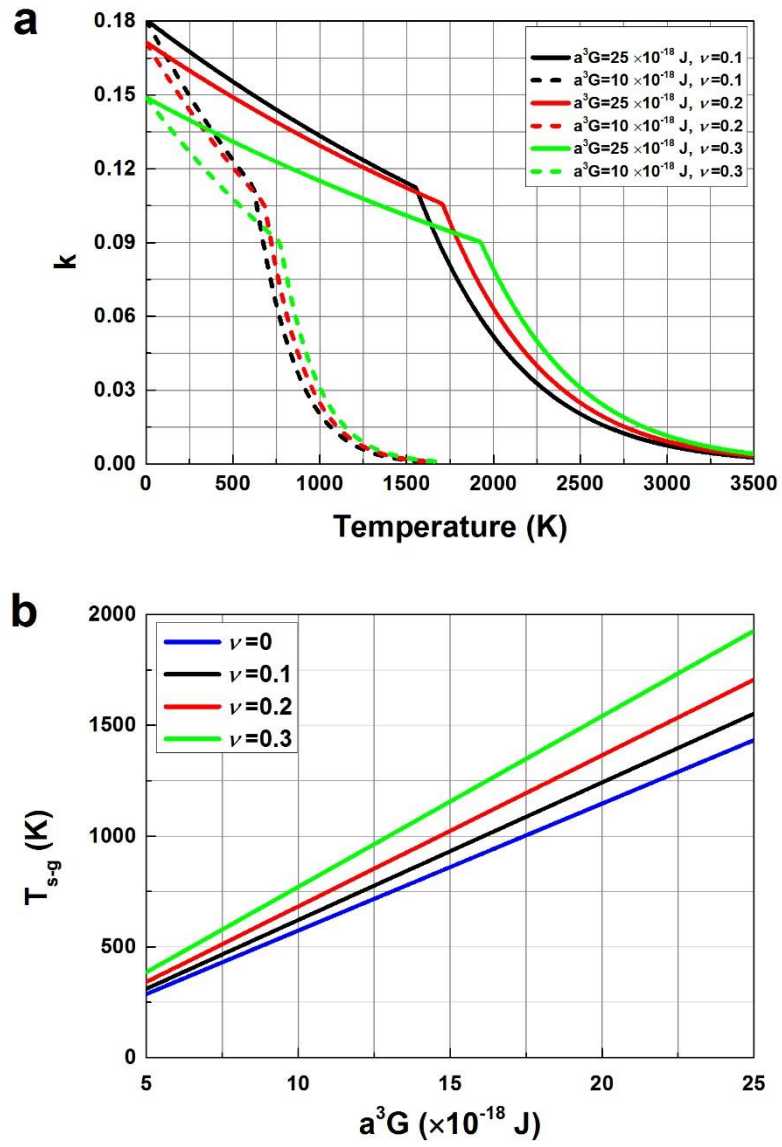


Fig. 4. Temperature effect on Vickers hardness of diamond-structured covalent materials. (a) The effects of temperature, a^3G , and Poisson's ratio on k . (b) The effect of a^3G and Poisson's ratio on the transition temperature T_{s-g} .

Supplemental Information

Temperature-dependent hardness of diamond-structured covalent materials

Xing Feng¹, Jianwei Xiao¹, Bin Wen^{1,*}, Jijun Zhao², Bo Xu^{1,†}, Yanbin Wang³, Yongjun Tian¹

¹ State Key Laboratory of Metastable Materials Science and Technology, Yanshan University, Qinhuangdao 066004, China

² Key Laboratory of Materials Modification by Laser, Ion and Electron Beams (Ministry of Education), Dalian University of Technology, Dalian 116024, China

³ Center for Advanced Radiation Sources, University of Chicago, Chicago, Illinois 60439, USA.

Part I. Molecular Dynamics method

The dislocation motion in diamond can be considered as a process of kink-pairs nucleation and migration, hence its activation energy is depending on kink-pair formation energy and kink migration energy barrier. To obtain activation energy for shuffle-set 0° perfect and glide-set 90° partial dislocation motion, a series of dislocation kink-pair structure models with different kink-pair widths are built. These structure model contains about 115,200 atoms, and their x, y, z axes are redefined along matrix's $[1\bar{1}\bar{2}]$, $[\bar{1}10]$, and $[111]$ directions of diamond. The constructed structure is optimized by using LAMMPS program [1], and C-C bonding interactions are described by LCBOP (Long-range Bond-order Potential for Carbon) potential [2]. Periodic boundary condition is only imposed along they y axis and free surface was imposed in x and z directions. After optimized, kink-pair formation energy (W_f) different kink-pair widths was obtained according to system energy variation, and the kink migration energy barrier (W_m) was obtained using Nudged Elastic Band (NEB) method [3]. Based on these calculated kink formation energy at different kink-pair widths and the corresponding kink migration energy barrier, activation energy for shuffle-set 0° perfect and glide-set 90° partial

Authors to whom any correspondence should be addressed

* E-mail address: wenbin@ysu.edu.cn (Bin Wen)

† E-mail address: bxu@ysu.edu.cn (Bo Xu)

dislocation motion was obtained by finding maximal total energy (addition of kink formation energy and kink migration energy barrier) with respect to kink-pair width [4].

Part II. First-principles method

First-principles calculations for these diamond-structured covalent materials are carried out in the framework of the density functional theory (DFT) [5,6] with the projector-augmented wave (PAW) [7] method, implemented in Vienna ab initio simulation package (VASP) [8-10]. The generalized gradient approximation (GGA) in the form of Perdew-Burke-Ernzerhof (PBE) [11] is used for the exchange-correlation potential. The plane-wave cutoff energy for all crystals is 500 eV, and the k -points is taken to be $15 \times 15 \times 15$ using the Monkhorst-Pack method. Forces on the ions are calculated according to the Hellmann-Feynman theorem, and the convergence thresholds for total energy and ionic force component are set to 1×10^{-6} eV and 0.001 eV/Å, respectively. The Debye frequencies are obtained as the maximum of phonon frequencies calculated by the finite displacement method implemented in the PHONOPY code [12].

Based on first-principles calculations, three independent elastic constants, i.e., C_{11} , C_{12} , and C_{44} for cubic crystal. According to the Voigt-Ruess-Hill approximations [13], the elastic moduli can be obtained based on the results of elastic constants. For cubic crystals, the Voigt and Reuss bulk modulus (B_V , B_R) and Voigt and Reuss shear modulus (G_V , G_R) can be given as

$$B_V = (C_{11} + 2C_{12})/3, \quad (S1)$$

$$B_R = (3S_{11} + 6S_{12})^{-1}, \quad (S2)$$

$$G_V = (C_{11} - C_{12} + 3C_{44})/5, \quad (S3)$$

$$G_R = 5(4S_{11} - 4S_{12} + 3S_{44})^{-1}, \quad (S4)$$

where S_{ij} are the elastic compliance constants (i.e., $S_{ij} = C_{ij}^{-1}$). Finally, the elastic moduli can be approximated by Hill's average, for bulk modulus $B = (B_V + B_R)/2$, and for shear modulus $G = (G_V + G_R)/2$. Further, the Poisson's ratio is given by

$$\nu = \frac{3B - 2G}{2(3B + G)}. \quad (\text{S5})$$

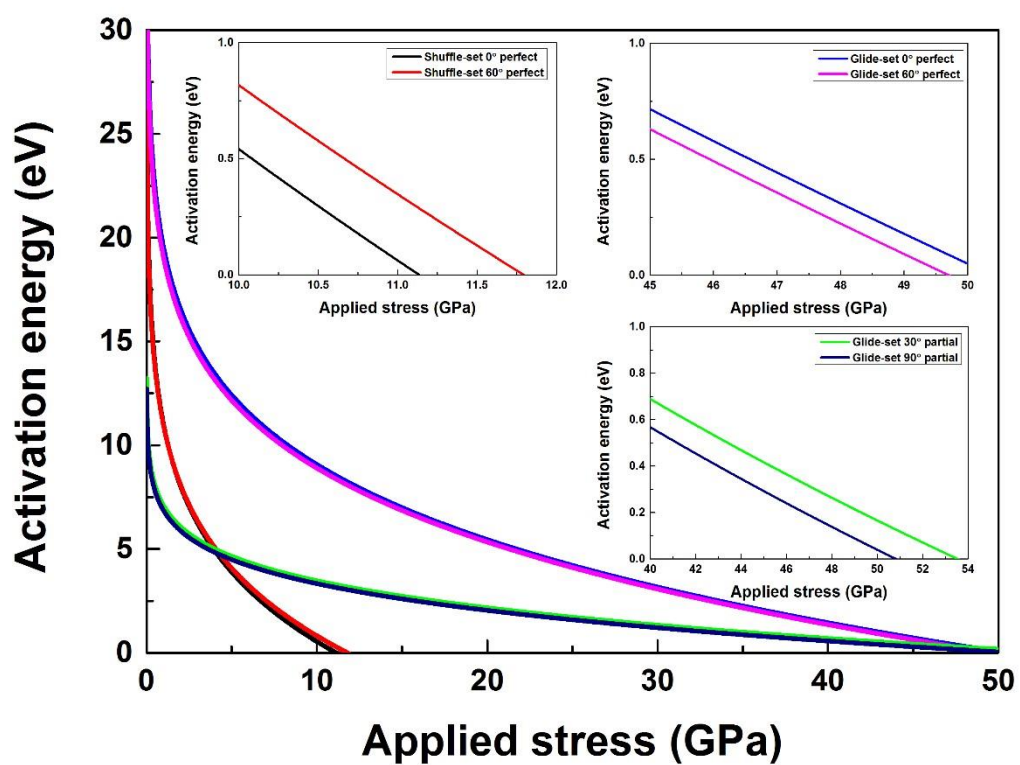


Fig. S1. Activation energy for six types of dislocations in diamond as a function of applied stress.

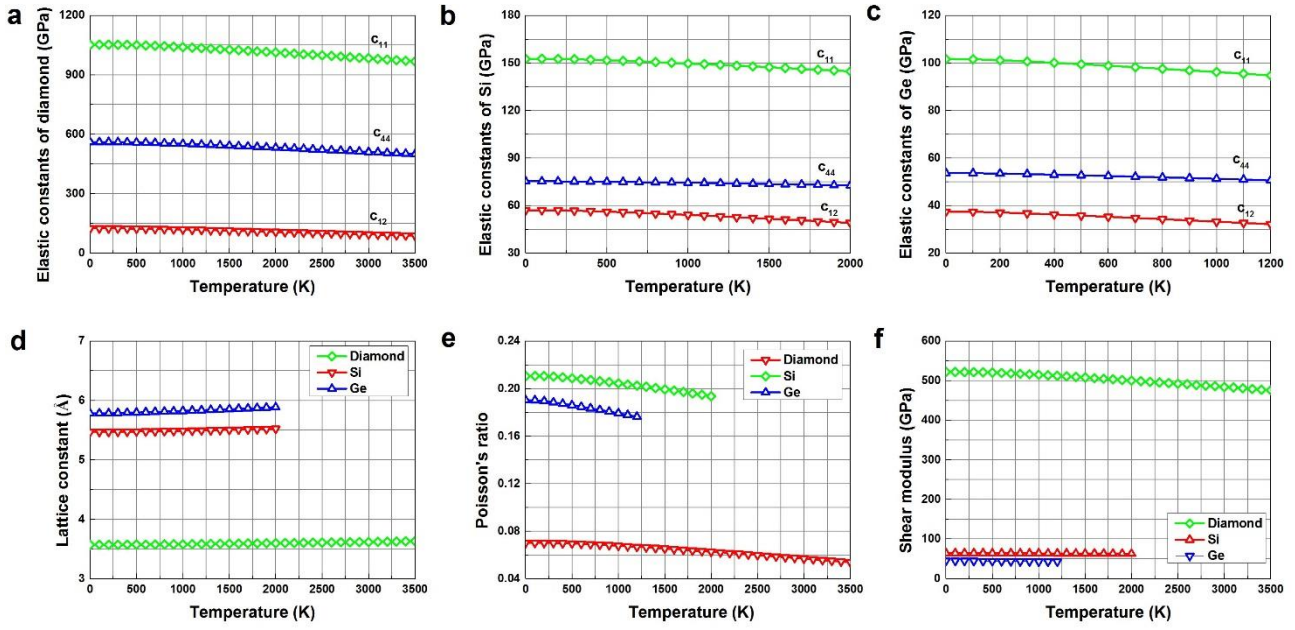


Fig. S2. Temperature-dependent elastic constants of diamond, Si and Ge. (a) temperature-dependent c_{11} , c_{12} and c_{13} of diamond. (b) temperature-dependent c_{11} , c_{12} and c_{13} of Si. (c) temperature-dependent c_{11} , c_{12} and c_{13} of Ge. (d) the optimized temperature-dependent lattice constant of diamond, Si and Ge. (e) the temperature-dependent Poisson's ratio of diamond, Si and Ge. (f) the temperature-dependent shear modulus of diamond, Si and Ge.

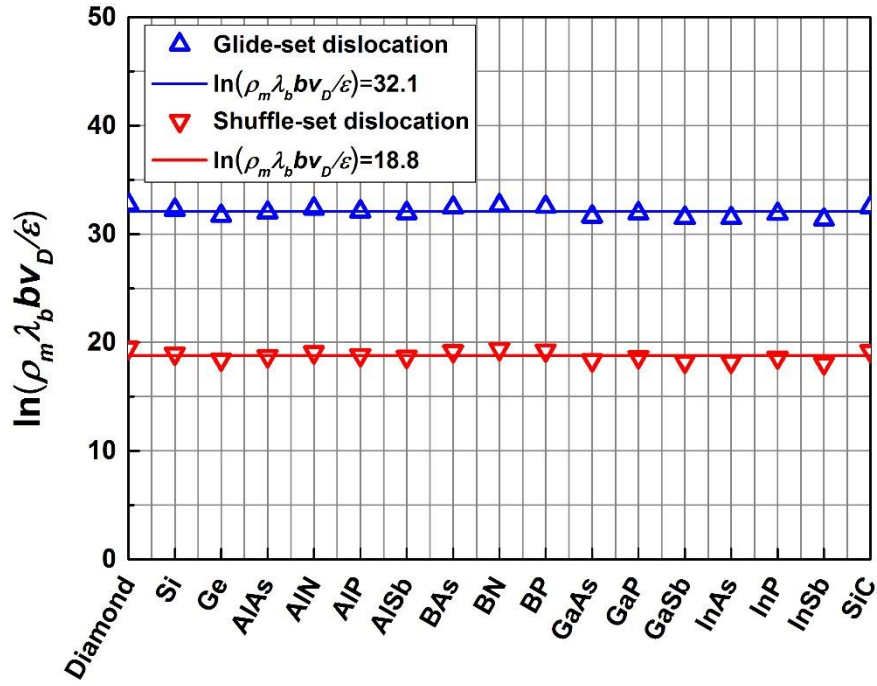


Fig. S3. Variation of $\ln(\rho_m \lambda_b b v_D / \dot{\epsilon})$ for glide-set and shuffle-set dislocations for selected diamond-structured covalent materials. In particular, $\dot{\epsilon} = 10^{-4} \text{ s}^{-1}$, $\rho_m^s = 0.3 \times 10^8 \text{ m}^{-2}$ and $\rho_m^g = 0.3 \times 10^{14} \text{ m}^{-2}$, $\lambda_b = 100 \text{ nm}$, and b and v_D is Burgers vector and Debye frequency for different diamond-structured covalent materials.

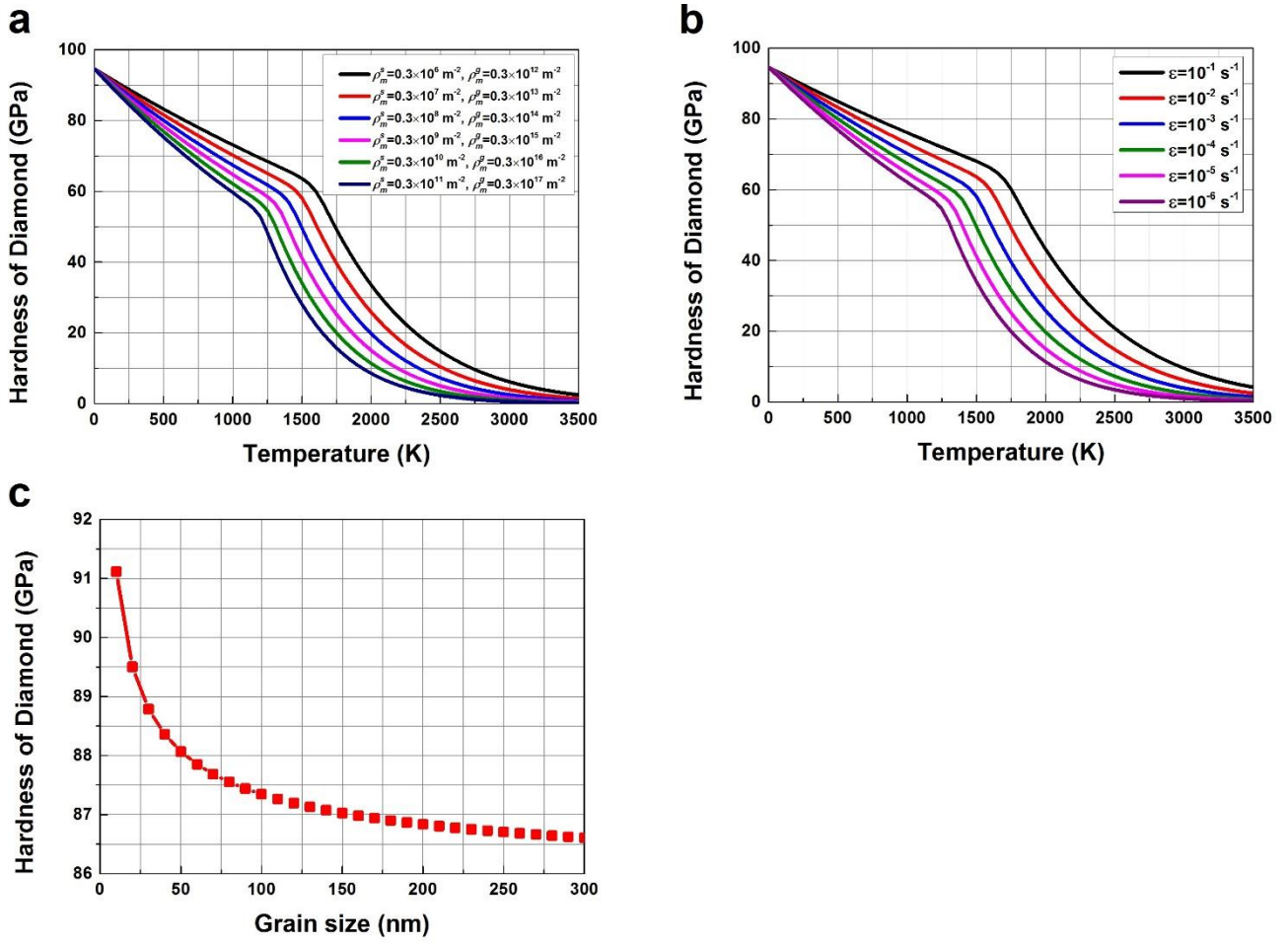


Fig. S4. (a) Effect of mobility of dislocation density on hardness of diamond. (b) Effect of strain rate on hardness of diamond. (c) Effect of grain size on hardness of diamond by considering the Hall-Petch effect.

References

- [1] S. J. Plimpton, *Fast Parallel Algorithms for Short-range Molecular Dynamic* (Academic Press Professional, Inc., 1995).
- [2] J. H. Los and A. Fasolino, *Physical Review B* **68**, 366 (2003).
- [3] Z. Ting, L. Ju, S. Amit, L. Austin, and G. Ken, *Physical Review Letters* **100**, 025502 (2008).
- [4] L. Pizzagalli, A. Pedersen, A. Arnaldsson, H. Jónsson, and P. Beauchamp, *Physical Review B* **77** (2012).
- [5] P. Hohenberg and W. Kohn, *Physical Review* **136**, B864 (1964).
- [6] W. Kohn and L. J. Sham, *Physical Review* **140**, A1133 (1965).
- [7] P. E. Blöchl, *Physical Review B* **50**, 17953 (1994).
- [8] G. Kresse and J. Furthmüller, *Computational Materials Science* **6**, 15 (1996).
- [9] G. Kresse and J. Furthmüller, *Physical Review B* **54**, 11169 (1996).
- [10] G. Kresse and D. Joubert, *Physical Review B* **59**, 1758 (1999).
- [11] J. P. Perdew, K. Burke, and M. Ernzerhof, *Physical Review Letters* **77**, 3865 (1996).
- [12] A. Togo, F. Oba, and I. Tanaka, *Physical Review B* **78**, 134106 (2008).
- [13] R. Hill, *Proceedings of the Physical Society* **65**, 349 (1952).